

Journal of Materials Chemistry A

Accepted Manuscript



This is an *Accepted Manuscript*, which has been through the Royal Society of Chemistry peer review process and has been accepted for publication.

Accepted Manuscripts are published online shortly after acceptance, before technical editing, formatting and proof reading. Using this free service, authors can make their results available to the community, in citable form, before we publish the edited article. We will replace this *Accepted Manuscript* with the edited and formatted *Advance Article* as soon as it is available.

You can find more information about *Accepted Manuscripts* in the [Information for Authors](#).

Please note that technical editing may introduce minor changes to the text and/or graphics, which may alter content. The journal's standard [Terms & Conditions](#) and the [Ethical guidelines](#) still apply. In no event shall the Royal Society of Chemistry be held responsible for any errors or omissions in this *Accepted Manuscript* or any consequences arising from the use of any information it contains.

Enhanced Absorbing Properties of Three-Phase Composites Based on Thermoplastic-Ceramic Matrix (BaTiO₃ +PVDF) and Carbon Black Nanoparticles

Xiao-Min Meng^{a,§}, Xiao-Juan Zhang^{b,§}, Chang Lu^b, Ya-Fei Pan^b, Guang-Sheng Wang^{b,*}

Received (in XXX, XXX) Xth XXXXXXXXX 20XX, Accepted Xth XXXXXXXXX 20XX

DOI: 10.1039/b000000x

The novel three-phase composites with excellent electromagnetic wave absorption properties based on the carbon black nanoparticles (CB) and BaTiO₃ (BT) nanoparticles embedded into polyvinylidene fluoride (PVDF) were prepared by using a simple blending and hot-molding technique. When the composites with filler content of CB 10wt.% and BT 5wt.% , the reflection loss of the composite can reach -38.8 dB at 9.2 GHz, and reflection loss of less than -10 dB in the frequency range is from 3.5 to 18.0 GHz with an absorber thickness of 1.5-5.0 mm. Compared with the two-phase composites of CB/PVDF and BT/PVDF composites, the three-phase composites showed more excellent absorption properties. The Debye relaxation theory was used to explain the enhanced absorption properties.

Introduction

At the beginning of this century, the electromagnetic wave in GHz range used in wireless telecommunication systems and high frequency circuit devices, such as mobile phone, local area network, satellite broadcast systems, et al. has been thought as the fourth pollution. And more and more attention has been paid towards finding suitable electromagnetic wave-absorbing materials to prevent this phenomena.¹⁻⁵ The basic design theories of radar absorbing materials (RAM), such as Salisbury screen theory, Jaumann absorber theory, etc. were published from early 1950s onwards. But these theoretical studies abated, recently, the main research topic being transferring toward the development of loss material⁶⁻⁹ and many methods have been studied to improve the reflection loss. Different methods have been used to improve the EM wave absorption efficiency and broaden the effective absorbing bands of the absorbers, such as adding optimized absorbent,¹⁰ compounding different types of absorbents,^{11, 12} using multi-layer structure.^{13, 14} It has been indicated that absorbers with nano-size, which have been investigated, possess wider wave absorption bandwidth and larger reflection loss (RL).^{15, 16} In previous study, as a typical kind of microwave absorption material, many nanostructures, such as CeO₂,¹⁷ CuS nanostructures,^{7, 8} β-MnO₂ nanorods,¹⁸ ZnO nanostructures,⁹ SiC fibers,¹⁹ 3D α-MnO₂²⁰ and MnFe₂O₄ nanoparticles²¹ have been reported. To date, much attention is being paid to carbon-based materials in EM wave absorption field, especially for carbon nanosheets and graphene nanocomposites.²²

However, from the existing reports that we can find,²³⁻²⁶ most of the composites are prepared by paraffin wax. As wax is a kind of soft material, possessing low melting point, which will restrict the practical application of materials immensely. To solve this problem, in our recent study, the paraffin wax was replaced by PVDF, which is a polymer with flexible properties and can be tailored to any shapes as you want.⁶⁻⁸ PVDF is chosen as composite polymeric matrix materials in the fabrication of

inorganic-organic nanocomposites also because of its specific physical properties and excellent dielectric properties,^{9, 18, 27-29} which can overcome the drawbacks of paraffin wax based composites. Besides, our research also revealed that existence of synergic effect between PVDF and nanofillers, which could distinctly enhance the wave-absorption of nanocomposite.

At the meantime, the synthesis of nanomaterials is complicated and their practical applications were restricted due to high cost and complicated preparation processes of fillers. CB-N550 as conductive powder is largely used owing to good absorption performance in higher frequency range,³⁰ meanwhile, it is light and cheap enough. And the BaTiO₃ was also selected as an absorber in recent report. For example, in our pervious study, the nano-size BT can also adjust the dielectric properties,²⁹ so the nano-size BaTiO₃ particles are also employed to improve the dielectric and wave absorption properties.

In this paper, we firstly prepared the (CB+BT)/PVDF composites by a simple blending method. Because of the existence of nano-size BT particles in composites, they would disperse in PVDF solution homogeneously and could not agglomerate together. The enhanced wave absorption of (CB+BT)/PVDF composites were also investigated.

Experimental

Commercially available and analytical-grade reagents were used without further purification. The CB-N550 was purchased from Shandong Jian'an Industrial Co., Ltd. And BT powder was purchased from Beijing Shengbogaotai Optical Technology Co., Ltd. The composites were prepared by mixing the BT powders (80-100 nm) with the polymer PVDF using a simple blending and hot-molding procedure. PVDF was dissolved in *N*-dimethylformamide (DMF) at room temperature. After the solution was transparent, various contents of Carbon Black were added and then dispersed in fosters after the ultrasonic bath at room temperature. After that, it was dried in the oven at 100 °C.

The dried mixture was collapsed and compressed into wafers for 15 min at 200 °C under 10 MPa (prepressed for 5 min at the same temperature, released the press for a while, and then repressed for 20 min, followed by cooling to room temperature under the same pressure).

Powder XRD data were collected on a Rigaku D/MAX 2200 PC automatic X-ray diffractometer with Cu K α radiation (λ) 0.154056 nm). The grain morphology and size was observed by SEM (FEI Siron 200). The relative permittivities were measured in the 2–18 GHz range with an Agilent E8363B network analyzer.

Results and discussion

A general SEM overview of the sample of Carbon Black particles was shown in Fig. 1a. It indicates that the product mainly consists of mono-dispersed particles with the diameter about 50-80 nm. The SEM image of BaTiO $_3$ nanoparticles was also given in the Fig. 1 b, from the image, it can be found that the product is mainly nanoparticles with the diameter about 100 nm.

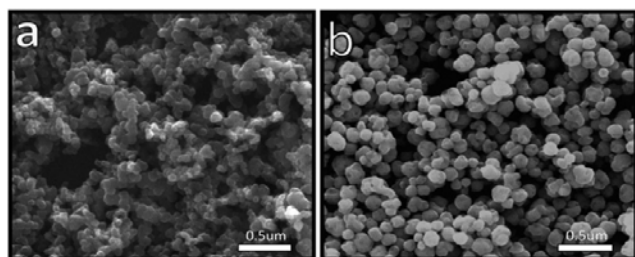


Fig. 1 SEM images of (a) the Carbon Black Particles and (b) BT nanoparticles

To investigate how the addition affect the dielectric properties of composites, various contents of CB or/and BT powders were mixed with PVDF to form BT/PVDF, CB/PVDF and (CB+BT)/PVDF composites by a hot-press process. For comparing, the CB and BT powders were also mixed with wax to form the CB/wax and BT/wax composites. The SEM image of composite in Fig. 2a indicates dispersion of BT and CB particles and compact structure in the polymer, from the SEM image, the interface between BT+CB particles and polymer was eliminated. The shape of the BT and CB particles is still kept in the composites after the hot-press. As shown in Fig. 2b, the elemental maps of Ba, O, and Ti, which are on the surface of the (CB+BT)/PVDF nanocomposites, also confirm the good dispersion of the BT in PVDF.

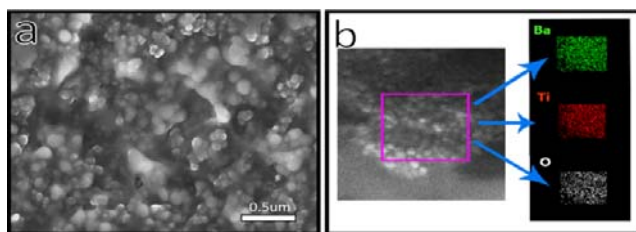


Fig. 2 (a) Cross-sectional FESEM images of the (CB+BT)/PVDF membrane; (b) the elemental maps of Ba, O, and Ti in the composites

To confirm the element of the composites, the XRD of pure PVDF, CB, BT and the composites of (CB+BT)/PVDF were shown in the Fig. 3. From the XRD pattern, the peaks of BT and the PVDF are still kept, which further confirmed the existed of BT in the composites, while the peak of CB disappeared due to the low filler content.

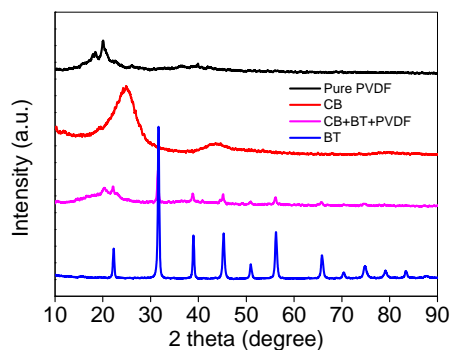


Fig. 3 XRD of pure PVDF, CB, BT and the (CB+BT)/PVDF membrane

The specimen for dielectric properties measurement using coaxial wire method were prepared by uniformly mixing the BT or/and CB in a paraffin matrix or PVDF which was transparent to EM waves and pressed the mixture into a cylindrical shaped compact (Φ_{out} =7.00 mm and Φ_{in} =3.04 mm). The relative permittivity ϵ' values were measured in the 2–18 GHz range with an Agilent E8363B network analyzer. The frequency dependency on the relative permittivity for all the composites, is shown in Fig. 4a. The curves indicate that all the real permittivity ϵ' decrease smoothly with the increasing frequency, except the CB/PVDF with the filler loading 20 wt.%, which decreases from 96 to 20 quickly at the range 2-6 GHz and then decrease with the increasing frequency; we think that this phenomena can be the same with the percolative composites at low frequency, and the polarization of molecules does not have enough time to catch up with the change of applied electrical field.³¹ As for the three phase (CB+BT)/PVDF composites, the real permittivity is higher than those of the BT in paraffin matrix and BT/PVDF in the all frequency, and the real permittivity also increase with the increase filler loading of BT and CB, which is the same with the previous result.²⁹ While, the curve of imaginary permittivity ϵ'' (shown in Fig. S1) shows the same variation tendency, respectively, it worth noted that the imaginary permittivity ϵ'' of CB/PVDF with the filler loading 20 wt.% keep higher than those of other composites, which can be helpful to get a high dielectric loss. Based on the data in Fig. 4a and Fig. S1, we also calculated

the dielectric loss tangent ($\tan \sigma = \frac{\epsilon''}{\epsilon'}$) which is shown in Fig. 4b, only dielectric tangent loss of the CB/PVDF exhibited a strong peaks at about 6.0 GHz and keep higher than those of other samples, which correspond to the peaks of imaginary permittivity ϵ'' , and the value of the dielectric tangent loss is higher than 1.4. As for the other composites, dielectric loss of the three phase (CB+BT)/PVDF composites is higher than those of the BT in paraffin matrix and BT/PVDF in the all frequency, and the real permittivity also increase with the increase filler loading of BT and CB; the dielectric loss of the (CB+BT)/PVDF composites with the CB and BT loading 10 wt.% and 5 wt.% are higher than 0.4 in the frequency range of 2-18 GHz, while, the (CB+BT)/PVDF composites with the CB and BT loading 20 wt.% and 10 wt.% is higher than 0.6, the high dielectric loss may result in the excellent reflection loss. The dielectric loss mechanism is mainly attributed to the relaxation process. And interfacial polarization is one of the most important relaxation process. In addition, PVDF is a strong dipole material due to the existence of electrophilic fluorine in its molecular structure. So it

may cause electronic dipole polarization, which is also beneficial
185 to dielectric loss.³¹

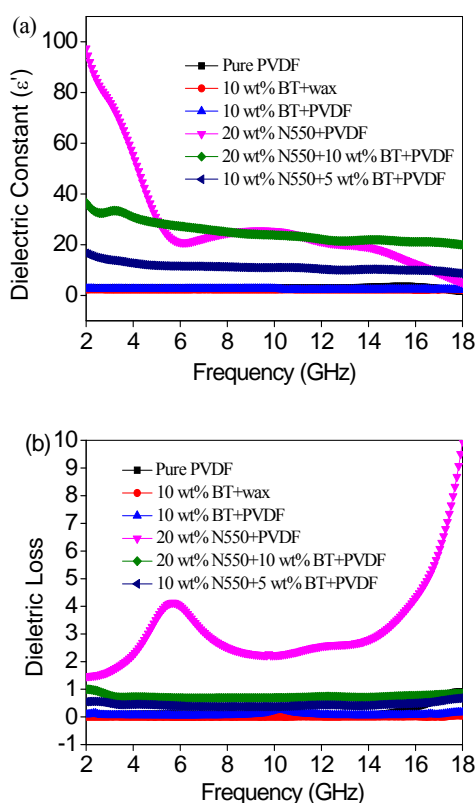


Fig. 4 Frequency dependence of the permittivity (a) and the dielectric loss (b) for the pure PVDF, BT/Wax, BT/PVDF, CB/PVDF and (CB+BT)/PVDF
190 composites

To study the microwave absorption, we calculated the reflection loss (RLs) of the electromagnetic radiation under the normal incidence of the electromagnetic field. The normalized input impedance (Z_{in}) is given by:³²

$$Z_{in} = \sqrt{\frac{\mu_r}{\epsilon_r}} \tanh \left[j \left(\frac{2f\pi d}{c} \right) \sqrt{\mu_r \epsilon_r} \right] \quad (1)$$

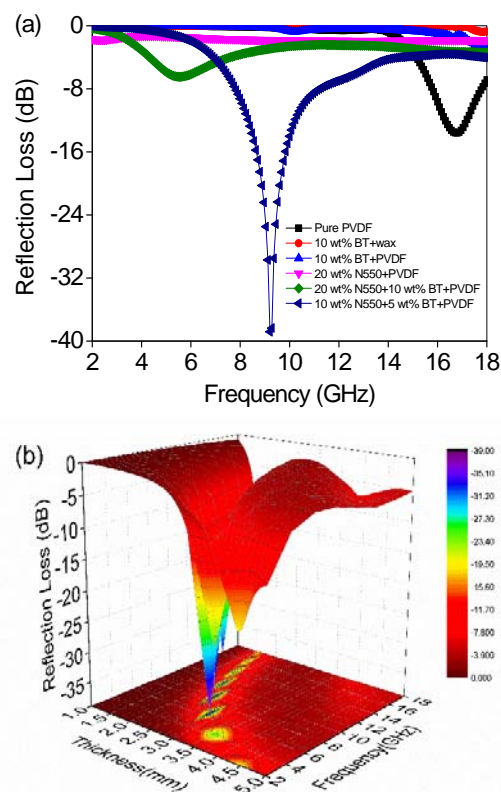
Where, ϵ_r and μ_r (for CB hexagonal platelet, μ_r is thought as 1),
200 are the complex permittivity and permeability of the composite absorber, respectively; f is the frequency; d is the thickness of the absorber, and c is the velocity of light in free space. The reflection loss (R) is related to Z_{in} as:³³

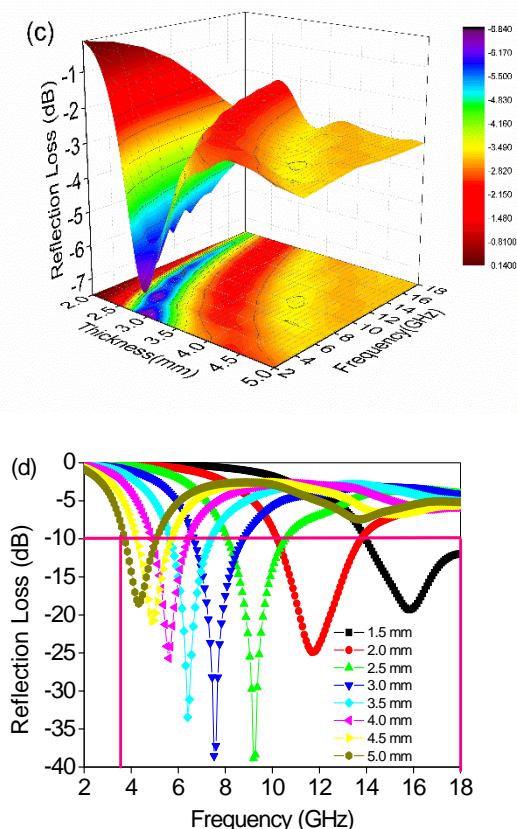
$$R = 20 \log \left| \frac{Z_{in} - 1}{Z_{in} + 1} \right| \quad (2)$$

Thus, the calculated RL of the composite absorbers with
205 different filler loadings under the same thickness 2.5 mm in the range of 2–18 GHz can be obtained through Eqs. (1) and (2) (shown in Fig. 5a). It can be observed that the composites with the different filler contents and the basic materials have a great influence on the microwave absorbing properties and the minimum RLs which correspond to the maximum absorptions. As for BT, with the same filler content, the BT/PVDF shows more excellent wave absorption property than the BT/wax; for comparing, the RL of BT/PVDF from 2-18 GHz was also given
210 in the Fig. S2. It is worth note that the RL of the (CB+BT)/PVDF composites is better than that of CB/PVDF, and the

(CB+BT)/PVDF composites with the loading content of CB 10 wt. % and BT 5wt. % shows more excellent RL value (-38.8 dB at 9.2 GHz) than that of the composites with the loading content
220 of CB 20 wt. % and BT 10wt. %. Moreover, as shown in Fig. 4b, it also confirms that sometimes high dielectric loss of absorber may result in weak absorption.⁸ In our composites, CB and BT particles are well dispersed in the PVDF, which will increase the dielectric loss; higher concentration of CB and BT particles may
225 result in higher conductivity, and bring into dielectric loss. Besides, high concentration of CB and BT particles in this composite also result in the occurrence of a significant skin effect as its surface is irradiated by microwave,^{34, 35} which cause damage to the wave-absorption of materials.

The three-dimensional presentations of RL were also shown in Fig. 5b, and c, the images displayed the calculated theoretical RLs of the (CB+BT)/PVDF composites with different thickness (2-5 mm) in the range of 2-18 GHz with the different loading, respectively. From the Fig. 5b and c, it indicates that the
230 microwave absorbing properties and the minimum RLs gradually appear in different frequency and can be tunable by controlling the thickness of the absorbers. The Fig. 5d also shows the excellent absorption performances of the (CB+BT)/PVDF composites with the loading content of CB 10 wt. % and BT 5 wt. % and the minimum RL can be adjusted by controlling the
240 thickness in the frequency range of 2-18 GHz. For comparison, the (CB+BT)/PVDF composites with filler CB 20wt %, BT 10wt.% in the frequency range of 2-18 GHz also calculated in Fig. S3. In addition, according to Fig. 5d, the (CB+BT)/PVDF composites
245 attained a reflection loss of less than -10 dB in the frequency range from 3.5 to 18.0 GHz with an absorber thickness of 1.5-5.0 mm, confirming that this kind of composite is a broadband wave-absorbing material,³⁶ which is quite beneficial to many electromagnetic shielding materials designed to reduce
250 electromagnetic waves over a wide frequency range.





255 **Fig. 5** (a) Microwave RL curves of the composites with a thickness of 2.5 mm; The three-dimensional presentations of RL of (CB+BT)/PVDF composites (b) and (c) at various thicknesses in the frequency range of 2-18 GHz with different loadings of CB 10wt. %, BT 5wt.% and CB 20wt. %, BT 10wt.%; (d) The microwave RL curves of (CB+BT)/PVDF composites with filler CB 10wt %
 260, BT 5wt.% at different thicknesses in the frequency range of 2-18 GHz.

The enhanced absorption mechanism is still not clear, but, for dielectric loss material to absorb microwave, Debye dipolar relaxation is an important mechanism. And the relative complex permittivity can be expressed by the following equation,³⁷

$$\epsilon_r = \epsilon_\infty + \frac{\epsilon_s - \epsilon_\infty}{1 + j2\pi f\tau} = \epsilon' - j\epsilon'' \quad (3)$$

where f , ϵ_s , ϵ_∞ , and τ are frequency, static permittivity, relative dielectric permittivity at the high-frequency limit, and polarization relaxation time, respectively. Thus, ϵ' and ϵ'' can be described by

$$\epsilon' = \epsilon_\infty + \frac{\epsilon_s - \epsilon_\infty}{1 + (2\pi f)^2 \tau^2} \quad (4)$$

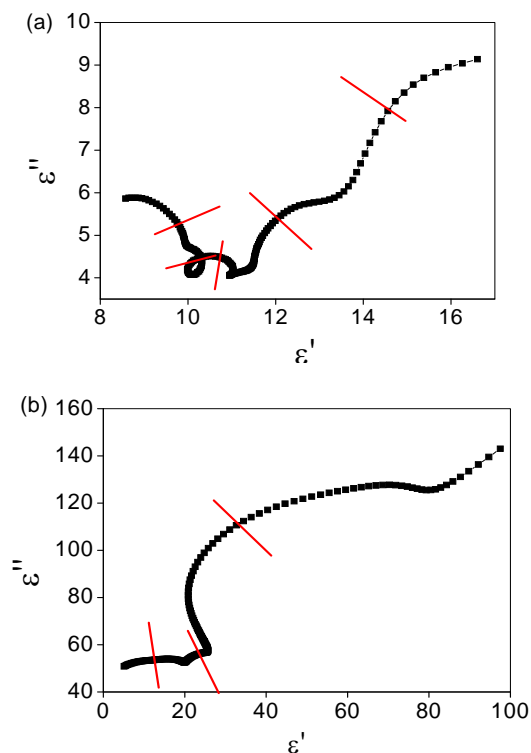
$$\epsilon'' = \frac{2\pi f\tau(\epsilon_s - \epsilon_\infty)}{1 + (2\pi f)^2 \tau^2} \quad (5)$$

According to eqn (4) and (5), the relationship between ϵ' and ϵ'' can be deduced,

$$\left(\epsilon' - \frac{\epsilon_s + \epsilon_\infty}{2}\right)^2 + (\epsilon'')^2 = \left(\frac{\epsilon_s - \epsilon_\infty}{2}\right)^2 \quad (6)$$

Thus, the plot of ϵ'' versus ϵ' would be a single semicircle, generally denoted as the Cole-Cole semicircle. Each semicircle corresponds to one Debye relaxation process.³⁸ To further explain the enhanced absorption properties, Fig. 6a and b show the ϵ'' - ϵ' curves of the (CB+BT)/PVDF composites with filler loading CB 10wt. %, BT 5 wt.% and CB/PVDF composites with

filler content of 20 wt.%, respectively. For the semicircles corresponding to the Debye relaxation process, the ϵ'' - ϵ' plot of composites exhibits a succession of semicircles, which can be ascribed to relaxation phenomena due to the contribution of grain (bulk), grain boundary and interface/electrode polarization. For pure PVDF, there is an obvious Cole-Cole semicircle in the ϵ'' - ϵ' curve (shown in the Fig. S4), indicating the existence of Debye relaxation process in the pure PVDF. However, five semicircles are clearly found in the curve of (CB+BT)/PVDF composites (shown in the Fig. 6a), representing the contribution of Debye relaxation process of CB, BT, PVDF and the interface polarization caused by interfaces existed between BT, CB and PVDF. As to the CB/PVDF composites, there are only three semicircles in the curve (shown in the Fig. 6b), that is the Debye relaxation process of CB, PVDF and the interface polarization caused by interfaces between PVDF and CB, which also confirms that the enhanced absorption is related to the number of the semicircles, that is the Debye relaxation process.³⁹ In our system, the synergistic effect between the PVDF and CB, BT is also helpful to enhance the wave absorption properties. Another reason should be considered, CB particle is a conductor, which can increase conductivity of the composites, and the increased filler content of CB in this composite will increase the conductivity of the composite. According to the free-electron theory $\epsilon'' \propto \sigma / 2\pi\epsilon_0 f$ (σ is the electrical conductivity), increased conductivity of composite could result in strong dielectric loss.⁴⁰ Except for dielectric loss, another important wave absorption mechanism is impedance matching characteristic. In general, too high permittivity of absorber is harmful to the impedance match and will result in strong reflection and weak absorption. That is why the (CB+BT)/PVDF composites with filler loading CB 10wt. %, BT 5 wt.% have more excellent wave absorption property than that of composites with filler loading CB 20wt. %, BT 10 wt.%.⁴¹



280 **Fig. 6** The ϵ'' - ϵ' curve of (CB+BT)/PVDF composites with filler loading CB 10 wt. %, BT 5wt.% (a) and CB/PVDF composites with CB 20 wt.% (b)

Conclusions

In this paper, three phase (CB+BT)/PVDF composites with enhanced absorption properties have been synthesized. The structure of the film was studied in detail and the dielectric properties were also investigated. The results indicate that the absorption properties of three phase (CB+BT)/PVDF composites can also reach -38.8 dB at 9.2 GHz, the enhanced mechanism was also explained. In our system, due to the interfaces and the synergistic effect between the PVDF, CB and BT, the enhanced absorption properties can be achieved. The (CB+BT)/PVDF composites possess excellent microwave absorption performance which is promising for applications in commercial, military and scientific electronic devices, and the method is also suitable for industrial production.

Acknowledgment. This project was financially supported by the National Natural Science Foundation of China (Nos. 51472012 and 51102223).

^aSchool of Chemical Engineering, Northeast Dianli University, Jilin 132000, PR China

^bKey Laboratory of Bio-Inspired Smart Interfacial Science and Technology of Ministry of Education, School of Chemistry and Environment, Beihang University, Beijing 100191, PR China.

wanggsh@buaa.edu.cn

[§] These authors are equal to this job.

[†] Electronic Supplementary Information (ESI) available: details of any supplementary information available should be included here. See DOI: 10.1039/b000000x/

Notes and references

1. Y. Ren, C. Zhu, S. Zhang, C. Li, Y. Chen, P. Gao, P. Yang and Q. Ouyang, *Nanoscale*, 2013, **5**, 12296-12303.
2. T. Xia, C. Zhang, N. A. Oylar and X. Chen, *Adv. Mater.*, 2013, **25**, 6905-6910.
3. J. Liu, R. Che, H. Chen, F. Zhang, F. Xia, Q. Wu and M. Wang, *Small*, 2012, **8**, 1214-1221.
4. W. Zhu, L. Wang, R. Zhao, J. Ren, G. Lu and Y. Wang, *Nanoscale*, 2011, **3**, 2862-2864.
5. J. Jiang, D. Li, D. Geng, J. An, J. He, W. Liu and Z. Zhang, *Nanoscale*, 2014, **6**, 3967-3971.
6. G.S. Wang, X.J. Zhang, Y.Z. Wei, S. He, L. Guo and M.S. Cao, *J. Mater. Chem. A*, 2013, **1**, 7031-7036.
7. X.J. Zhang, G.S. Wang, Y.Z. Wei, L. Guo and M.S. Cao, *J. Mater. Chem. A*, 2013, **1**, 12115-12122.
8. S. He, G.S. Wang, C. Lu, J. Liu, B. Wen, H. Liu, L. Guo and M.S. Cao, *J. Mater. Chem. A*, 2013, **1**, 4685-4692.
9. G.S. Wang, Y.Y. Wu, X.J. Zhang, Y. Li, L. Guo and M.S. Cao, *J. Mater. Chem. A*, 2014, **2**, 8644-8651.
10. L. Liu, Y. Duan, S. Liu, L. Chen and J. Guo, *J. Magn. Magn. Mater.*, 2010, **322**, 1736-1740.
11. Y. Li, C. Chen, X. Pan, Y. Ni, S. Zhang, J. Huang, D. Chen and Y. Zhang, *Phys. B*, 2009, **404**, 1343-1346.
12. H. Yang, M. Cao, Y. Li, H. Shi, Z. Hou, X. Fang, H. Jin, W. Wang and J. Yuan, *Adv. Optical Mater.*, 2014, **2**, 214-219.
13. H. Xiong, J.S. Hong, C.M. Luo and L.L. Zhong, *J. Appl. Phys.*, 2013, **114**, 064109.
14. M. Cao, J. Zhu, J. Yuan, T. Zhang, Z. Peng, Z. Gao, G. Xiao and S. Qin, *Mater. Des.*, 2002, **23**, 557-564.
15. G. Wang, Z. Gao, S. Tang, C. Chen, F. Duan, S. Zhao, S. Lin, Y. Feng, L. Zhou and Y. Qin, *ACS Nano*, 2012, **6**, 11009-11017.
16. J. Zhan, Y. Yao, C. Zhang and C. Li, *J. Alloys Compd.*, 2014, **585**, 240-244.
17. H. Wu, L. Wang, Y. Wang and S. Guo, *Appl. Surf. Sci.*, 2012, **258**, 10047-10052.
18. G.S. Wang, L.Z. Nie and S.H. Yu, *RSC Adv.*, 2012, **2**, 6216-6221.
19. D. Ding, W. Zhou, B. Zhang, F. Luo and D. Zhu, *J. Mater. Sci.*, 2010, **46**, 2709-2714.
20. G.S. Wang, S. He, X. Luo, B. Wen, M.M. Lu, L. Guo and M.S. Cao, *RSC Adv.*, 2013, **3**, 18009-18015.
21. X.J. Zhang, G.S. Wang, W.Q. Cao, Y.Z. Wei, J.F. Liang, L. Guo and M.S. Cao, *ACS Appl. Mater. Interfaces*, 2014, **6**, 7471-7478.
22. B. Wen, M. Cao, M. Lu, W. Cao, H. Shi, J. Liu, X. Wang, H. Jin, X. Fang, W. Wang and J. Yuan, *Adv. Mater.*, 2014, **26**, 3484-3489.
23. X. Yuan, L. Cheng, L. Kong, X. Yin and L. Zhang, *J. Alloys Compd.*, 2014, **596**, 132-139.
24. S. J. Yan, S. L. Dai, H. Y. Ding, Z. Y. Wang and D. B. Liu, *J. Magn. Magn. Mater.*, 2014, **358-359**, 170-176.
25. R. Li, T. Wang, G. Tan, W. Zuo, J. Wei, L. Qiao and F. Li, *J. Alloys Compd.*, 2014, **586**, 239-243.
26. X. a. Fan, J. Guan, Z. Li, F. Mou, G. Tong and W. Wang, *J. Mater. Chem.*, 2010, **20**, 1676-1682.
27. G. Wang, Y. Deng, Y. Xiang and L. Guo, *Adv. Funct. Mater.*, 2008, **18**, 2584-2592.
28. G. Wang, Y. Deng and L. Guo, *Chem. - Eur. J.*, 2010, **16**, 10220-10225.
29. G. Wang, *ACS Appl. Mater. Interfaces*, 2010, **2**, 1290-1293.
30. A. A. Barba, G. Lamberti, M. d'Amore and D. Acierno, *Polym. Bull.*, 2006, **57**, 587-593.
31. X.J. Zhang, G.S. Wang, W.Q. Cao, Y.Z. Wei, M.S. Cao and L. Guo, *RSC Adv.*, 2014, **4**, 19594-19601.
32. L. Kong, X. Yin, Y. Zhang, X. Yuan, Q. Li, F. Ye, L. Cheng and L. Zhang, *J. Phys. Chem. C*, 2013, **117**, 19701-19711.
33. J. Guo, H. Wu, X. Liao and B. Shi, *J. Phys. Chem. C*, 2011, **115**, 23688-23694.
34. E. R. Cooper, C. D. Andrews, P. S. Wheatley, P. B. Webb, P. Wormald and R. E. Morris, *Nature*, 2004, **430**, 1012-1016.
35. Y.J. Chen, F. Zhang, G.G. Zhao, X.Y. Fang, H.B. Jin, P. Gao, C.L. Zhu, M.S. Cao and G. Xiao, *J. Phys. Chem. C*, 2010, **114**, 9239-9244.
36. X. Luo, G.S. Wang, H.Y. Guo, X.J. Zhang, W.Q. Cao, Y.Z. Wei, L. Guo and M.S. Cao, *ChemPlusChem*, 2014, **79**, 1089-1095.
37. J. Guo, X. Wang, X. Liao, W. Zhanga and B. Shi, *J. Phys. Chem. C*, 2012, **116**, 8188-8195.
38. B. Wen, M.S. Cao, Z.L. Hou, W.L. Song, L. Zhang, M.M. Lu, H.B. Jin, X.Y. Fang, W.Z. Wang and J. Yuan, *Carbon*, 2013, **65**, 124-139.
39. M.S. Cao, J. Yang, W.L. Song, D.Q. Zhang, B. Wen, H.B. Jin, Z.L. Hou and J. Yuan, *ACS Appl. Mater. Interfaces*, 2012, **4**, 6949-6956.
40. M.M. Lu, W.Q. Cao, H.L. Shi, X.Y. Fang, J. Yang, Z.L. Hou, H.B. Jin, W.Z. Wang, J. Yuan and M.S. Cao, *J. Mater. Chem. A*, 2014, **2**, 10540-10547.
41. M. Cao, R. Qin, C. Qiu and J. Zhu, *Mater. Des.*, 2003, **24**, 391-396.
42. C. Wang, X. Han, P. Xu, X. Zhang, Y. Du, S. Hu, J. Wang and X. Wang, *Appl. Phys. Lett.*, 2011, **98**, 072906.

Graphical Abstract

Three phase (CB+BT)/PVDF composites with enhanced absorption properties have been synthesized. The results indicate that the absorption properties of three phase (CB+BT)/PVDF composites also reach -38.8 dB at 9.2 GHz, the enhanced mechanism was also explained.

